Accepted Manuscript

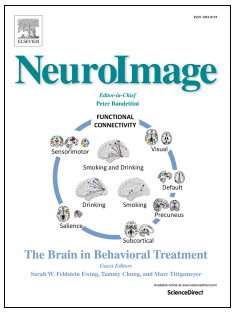

Consistency and similarity of MEG- and fMRI-signal time courses during movie viewing

Kaisu Lankinen, Jukka Saari, Yevhen Hlushchuk, Pia Tikka, Lauri Parkkonen, Riitta Hari, Miika Koskinen

PII: S1053-8119(18)30142-3

DOI: 10.1016/j.neuroimage.2018.02.045

Reference: YNIMG 14746

To appear in: *NeuroImage*

Received Date: 7 August 2017

Revised Date: 20 February 2018

Accepted Date: 22 February 2018

Please cite this article as: Lankinen, K., Saari, J., Hlushchuk, Y., Tikka, P., Parkkonen, L., Hari, R., Koskinen, M., Consistency and similarity of MEG- and fMRI-signal time courses during movie viewing, *NeuroImage* (2018), doi: 10.1016/j.neuroimage.2018.02.045.

Consistency and similarity of MEG- and fMRI-signal time courses during movie viewing

Kaisu Lankinen[1,2*], Jukka Saari[1], Yevhen Hlushchuk[3,4], Pia Tikka[3], Lauri Parkkonen[1], Riitta Hari[1,5], Miika Koskinen[1,6]

[1]*Department of Neuroscience and Biomedical Engineering, School of Science, Aalto University, P.O. Box 12200, FI-00076 AALTO, Finland*

[2]*Aalto NeuroImaging (AMI Centre and MEG Core), Aalto University, FI-00076 AALTO, Finland*

[3]*Department of Film, Television and Scenography, School of Arts, Design and Architecture, Aalto University, P.O. Box 16500, FI-00076 AALTO, Finland*

[4]*Department of Radiology, Hospital District of Helsinki and Uusimaa (HUS), HUS Medical Imaging Center, Helsinki University Central Hospital (HUCH), University of Helsinki, Helsinki, Finland*

[5]*Department of Art, School of Arts, Design and Architecture, Aalto University, P.O. Box 31000, FI-00076 AALTO, Finland*

[6]*Department of Physiology, Faculty of Medicine, P.O. Box 63, FI-00014 University of Helsinki, Finland*

Corresponding author:

Kaisu Lankinen

kaisu.lankinen@aalto.fi

Tel. +358 40 8659875

Fax: +358 9 47022969

Running title: fMRI and MEG during movie viewing

Submitted to Neuroimage

Abstract

Movie-viewing allows human perception and cognition to be studied in complex, real-life-like situations in a brain-imaging laboratory. Previous studies with functional magnetic resonance imaging (fMRI) and with magneto- and electroencephalography (MEG/EEG) have demonstrated consistent temporal dynamics of brain activity across movie viewers. However, little is known about the similarities and differences of fMRI and MEG/EEG dynamics during such naturalistic situations.

We thus compared MEG and fMRI responses to the same 15-min black-and-white movie in the same eight subjects who watched the movie twice during both MEG and fMRI recordings. We analyzed intra- and intersubject voxel-wise correlations within each imaging modality as well as the correlation of the MEG envelopes and fMRI signals. The fMRI signals showed voxel-wise within- and between-subjects correlations up to $r = 0.66$ and $r = 0.37$, respectively, whereas these correlations were clearly weaker for the envelopes of band-pass filtered (7 frequency bands below 100 Hz) MEG signals (within-subjects correlation $r < 0.14$ and between-subjects $r < 0.05$). Direct MEG–fMRI voxel-wise correlations were unreliable. Notably, applying a spatial-filtering approach to the MEG data uncovered consistent canonical variates that showed considerably stronger (up to $r = 0.25$) between-subjects correlations than the univariate voxel-wise analysis. Furthermore, the envelopes of the time courses of these variates below 11 Hz showed association with fMRI signals in a general linear model. Similarities between envelopes of MEG canonical variates and fMRI voxel time-courses were seen mostly in occipital, but also in temporal and frontal brain regions, whereas the strongest intra- and

intersubject correlations for MEG and fMRI separately were strongest only in the occipital areas.

In contrast to the conventional univariate analysis, the spatial-filtering approach was able to uncover associations between the MEG envelopes and fMRI time courses, shedding light on the similarities of hemodynamic and electromagnetic brain activity during movie-viewing.

Keywords

magnetoencephalography, functional magnetic resonance imaging, naturalistic stimulation, movie, intersubject correlation, canonical correlation analysis

1 Introduction

A practical and ecologically valid approach to probe the neural underpinnings of perception and social cognition is to use movies as stimuli in neuroimaging experiments. Mimicking everyday situations around us, movies can provoke a wide spectrum of sensory, social, and emotional percepts that may be difficult to elicit using the highly controlled repetitive stimuli typically employed in such experiments. Despite the apparent complexity and unrestrained nature of movies, consistent and synchronized brain activity patterns across movie viewers have been demonstrated with functional magnetic resonance imaging (fMRI; e.g. Hasson et al., 2004, Bartels and Zeki, 2004a; Bartels and Zeki, 2004b; Hasson et al., 2008; Jääskeläinen et al., 2008; Lahnakoski et al., 2012; Nummenmaa et al., 2012; Pamilo et al., 2012; Kauttonen et al., 2015), and more recently with magnetoencephalography (MEG;

Betti et al., 2013; Lankinen et al., 2014; Chang et al., 2015; Lankinen et al., 2016) and electroencephalography (EEG; Whittingstall et al., 2010; Dmochowski et al., 2012; Dmochowski et al., 2014; Bridwell et al., 2015; Chang et al., 2015; Ki et al., 2016; Cohen et al., 2016).

The fMRI and MEG signals often behave differently, reflecting the different physiological phenomena they measure (see for example Hari 2007; Hari and Kujala, 2009). BOLD (blood oxygenation level-dependent) signal in fMRI relates to hemodynamics and is sensitive to long-lasting activations in the range of seconds (Logothetis et al., 2001). MEG records directly the electromagnetic fields associated with synchronous activity of neuronal populations, and it picks up transient and sustained evoked activity as well as brain rhythms with millisecond-range temporal resolution (Hari & Puce, 2017). Moreover, both the onset and offset of a prolonged stimulus can elicit prominent transient responses in MEG, whereas BOLD builds up and fades away more sluggishly. It has been recently suggested that fMRI would receive the main contribution from neuronal ensembles connected via slow and thin fibres whereas MEG and EEG emphasize activity mediated by the fast-conducting pathways (Hari and Parkkonen, 2015).

The majority of previous comparisons between hemodynamic (fMRI) and electromagnetic (MEG or EEG) signals have used highly-controlled experimental designs with simplified and repeated stimuli (for a review, see e.g. Hall et al., 2014). Evidently, such settings fail to approximate neuronal activity occurring during real-world experiences. Instead, movies as continuous sequences of events unfolding over time may engage brain regions that show little responsivity in conventional experimental settings (e.g. Hasson et al., 2010).

In brain-imaging studies utilizing naturalistic stimuli, the analysis is often based on intersubject correlation (Hasson et al., 2004) that has been used for assessing the reliability and consistency of voxel-wise fMRI time courses during movie viewing (see e.g. Jääskeläinen et al., 2008; Golland et al., 2010; Kauppi et al., 2010; Nummenmaa et al., 2012; Lahnakoski et al., 2012; Kauppi et al., 2017). Compared with the strong across-viewers correlations in BOLD signals (up to 0.78 in Kauppi et al., 2010), the correspondingly calculated intersubject correlations of MEG or EEG signals are usually weaker (typically less than 0.1) both at sensor (Bridwell et al., 2015) and source level (Suppanen, E., 2014; Chang et al., 2015). However, calculating intersubject correlations in short sliding time windows have resulted in stronger correlation also for MEG and EEG signals (up to 0.5 within 200-ms sliding windows in Chang et al. (2015) and 0.3 within 5-s sliding windows in Dmochowski et al. (2012)). Here we assess intra- and intersubject correlations of MEG signals for a dense source space for the entire duration of a movie, calculated in the same manner as for fMRI.

An obvious challenge in the analysis of EEG or MEG data is the low signal-to-noise ratio (SNR), especially for unaveraged, single-trial traces recorded during naturalistic experiments (Dmochowski et al., 2012; Suppanen, E., 2014; Bridwell et al., 2015; Chang et al., 2015). With conventional well-controlled stimuli, the brain signals' SNR is typically improved by averaging the responses to repeated stimuli, which, however, is not practical in lengthy naturalistic experimental settings, such as movie-viewing.

Here we examine the feasibility of voxel-wise intra- and intersubject correlation analysis in MEG, and we extend our scrutiny to correlations between multivariate datasets. Previously, we have demonstrated the effectiveness of data-driven learning

of spatial-filter coefficients by multi-set canonical correlation analysis (MCCA; Kettenring, 1970; Li et al., 2009) to uncover signals that maximize intersubject correlation in MEG data between subjects (Lankinen et al., 2014). Notably, maximizing intersubject correlation also improves SNR of the signals. Previously, CCA and its derivatives have been used to maximize intersubject correlation in response to shorter videos or shorter movie clips in EEG recordings (Dmochowski et al., 2012; Dmowchowski et al., 2014; Ki el al., 2016; Cohen et al., 2016) that provide coarser spatial resolution than does MEG.

We conducted a systematic analysis between fMRI and MEG signals collected from the same subjects who were watching a 15-min movie. We used a silent black-and-white movie ”At Land” by Maya Deren as a naturalistic stimulus to study brain activity related to visual perception of real-world scenes.

Our analysis started from the assessment of (*i*) intra- and (*ii*) intersubject voxel-wise correlations separately for fMRI and MEG, (*iii*) extending to MEG–fMRI comparisons. Then, (*iv*) we proceeded from univariate to multivariate analysis and applied spatial-filtering with MCCA. Finally, (*v*) the resulting MEG canonical variates were associated with the fMRI voxel time series by a general linear model (GLM).

We demonstrate the usefulness of the proposed multivariate approach in relating MEG and fMRI signals in naturalistic experimental settings, in comparison to the more commonly used voxel-wise approach. Our findings show similarities in hemodynamic and electromagnetic brain activity in occipital, temporal and frontal brain regions during movie-viewing.

2 Materials and methods

2.1 Subjects

Eight healthy adults (4 females, 4 males; mean age 29 years, range 23–51 years) participated in the study. All subjects had normal or corrected-to-normal vision. Both the MEG and fMRI recordings had a prior approval by the ethics committee of Helsinki and Uusimaa Hospital district. All participants gave written informed consent prior to the study.

2.2 Stimulation

The subjects watched a 15-min silent black-and-white film “At Land” by Maya Deren (1944) twice during fMRI recordings and twice during MEG recordings. For each subject, the fMRI recording was performed first, and the MEG recording about one and a half year later. The film contained rich visual information of human bodily activities, especially the bodily behavior of the main character in her natural environment. Importantly, the film was originally directed as a silent film. Furthermore, since the film is not overloaded with dramatic narrative content, it suited well for our study interests as our focus was in brain activity related to visual perception and not on narrative comprehension.

In fMRI recordings, the movie was shown using Presentation software (version 0.81, http://www.neurobehavioralsystems.com) and projector Vista X3 REV Q (Christie Digital Systems, Canada, Inc.). The movie was projected to a semi-transparent back-projection screen that the subjects viewed via a mirror (visual angle 36° horizontal, 29° vertical). In MEG recordings, the screen was located 130 cm in

front of the subject (visual angle 22° horizontal, 17° vertical) and Experiment Builder software (SR Research, http://www.sr-research.com/eb. html) was used for playing the movie. The frame rate of the movie was 24 frames/s. For accurate temporal alignment between the movie playback and MEG recording, the stimulus presentation software was programmed to provide trigger signals to the MEG acquisition system at the beginning and end of the movie. The temporal jitter across subjects was within two sample periods (2 ms).

2.3 MRI and fMRI recordings

T1-weighted anatomical MRIs and the fMRI data were acquired using a 3.0 T General Electric Signa Scanner (General Electric, Milwaukee, WI, USA) at the Advanced Magnetic Imaging Centre of Aalto University. Structural images were scanned with 3-D T1 spoiled-gradient imaging, matrix 256 × 256, TR 10 ms, TE 3 s, flip angle 15°, preparation time 300 ms, FOV 25.6 cm, slice thickness 1 mm, voxel size 1 × 1 × 1 mm^3, and number of excitations 1. The functional images were acquired using a gradient echo-planar-imaging with following parameters: TR 2.015 s, TE 32 ms, flip angle 75°, 34 oblique axial slices, slice thickness 4 mm, matrix 64 × 64, voxel size 3.4 × 3.4 × 4 mm^3, field of view (FOV) 22 cm.

Four dummy scans were removed from the beginning of the recordings. Standard preprocessing steps—realignment, slice-time correction, coregistration of functional images to anatomical MRI, normalization and smoothing with an 8-mm full-width-at-half-maximum Gaussian kernel—were applied to the functional images with SPM8 toolbox (http://www.fil.ion.ucl.ac.uk).

2.4 MEG recordings

MEG was recorded with a 306-channel neuromagnetometer (Elekta Neuromag, Elekta Oy, Helsinki, Finland); the device houses 102 sensor units, each with two orthogonal planar gradiometers and one magnetometer. The acquisition passband was 0.03–330 Hz and the sampling rate 1000 Hz. Vertical and horizontal electro-oculograms (EOGs) were recorded at the same time. An additional 2-min recording with no subject present was performed on the same day for noise-covariance estimation.

2.4.1 MEG preprocessing

MEG data were preprocessed to suppress external magnetic interference by signal-space separation (SSS) method (Taulu and Kajola, 2005) implemented in Maxfilter software version 2.2 (Elekta Oy, Helsinki, Finland). Default parameter settings of the software were used and the data were converted into the standard head position.

The data were then further filtered and downsampled. Filtering was performed with a zero-phase FIR filter into 7 frequency bands: < 1, 1–4, 4–8, 8–11, 13–23, 25–45, and 55–100 Hz (with transition bands of 0.1 Hz for bands below 1 Hz, 0.5 Hz below 23 Hz, and 5 Hz below 100 Hz). After downsampling, the sampling frequencies were 50 Hz for the band below 1 Hz, 100 Hz for the band 1–11 Hz, 200 Hz for the band 13–45 Hz and 250 Hz for the band 55–100 Hz.

Eye-movement and eye-blink artifacts were suppressed by multiple linear regression applied to the MEG data by using the EOG signals as regressors in consecutive non-overlapping 60-s time windows. For validation, correlation between

the EOG signals and the MEG channels after EOG suppression was calculated in consequent non-overlapping 20-s windows separately for both EOG channels, and *t*-test was applied to find out if the mean of the correlations deviated from zero. For Bonferroni correction, the significance level was $p < 0.05/N_{channels}$.

2.4.2 MEG source analysis

We extracted the time series of cortical MEG sources using the minimum-norm estimation (MNE) method (Hämäläinen and Ilmoniemi, 1994) implemented in the MNE software package (Gramfort et al., 2014). For each subject, the T1-weighted magnetic resonance image of the brain was segmented and the cortical surface was reconstructed using FreeSurfer software (Dale et al., 1999; Fischl et al., 1999a, 1999b, Segonne et al., 2004) with the parameters described in default settings in the recommended reconstruction workflow in FreeSurferWiki

http://surfer.nmr.mgh.harvard.edu/fswiki/RecommendedReconstruction.

A single-compartment boundary element model (BEM) was applied and the MNEs were calculated using dipoles oriented normal to the cortical surface at discrete locations separated approximately by 6 mm (using icosahedron subdivision with parameter ‘4’) on the cortical surface, resulting in 5124 source signals in total. All 306 MEG channels were used in computing the MNEs.

Subject-specific source spaces were morphed to a common template ('fsaverage' in the FreeSurfer software package) for intersubject analysis. The resulting time courses of the MEG sources were further Hilbert-transformed to obtain the envelopes for each frequency band, low-pass filtered at 4 Hz and downsampled to 10 Hz to minimize computational load. For the MEG–fMRI comparison, the MEG envelopes were further convolved with the canonical hemodynamic response function (HRF;

SPM8 package; Wellcome Trust Centre for Neuroimaging; http://www.fil.ion.ucl.ac.uk/spm/software/spm8/). To avoid spurious boundary effects in filtering, 30 s of data were removed from both ends of the signals before calculating the correlations between the source-point time series. For simplicity, we will hereafter use the term "voxel-wise" also to refer to MEG time series at the source points.

2.4.3 MEG spatial-filtering with MCCA

Recently, we have proposed a spatial-filtering approach based on multi-set canonical correlation analysis (MCCA; Kettenring, 1971; Li et al., 2009) to uncover consistent brain signals across subjects (Lankinen et al., 2014).

Spatial-filtering refers to projection $\mathbf{Y}^m = \mathbf{W}^m\mathbf{Z}^m$, where the output $\mathbf{Y}^m$ is a weighted sum of the multidimensional signal $\mathbf{Z}^m$ ($D \times t$ matrix, where D is the dimension of the signals, and t the number of time points). Here, the supercript m refers to the dataset of one subject ($m = 1 \ldots M$, the number of subjects). The resulting projections in rows of $\mathbf{Y}^m$ ($D \times t$ matrix), i.e. the canonical variates, are mutually uncorrelated but maximally correlated between the subjects. Here, spatial filter weights $\mathbf{W}^m$ in MCCA were calculated by using MAXVAR cost function. In our analysis, the number of resulting projections is D = 68, corresponding to the remaining degrees of freedom (rank) of the data matrix after the SSS interference suppression method. We used PCA to reduce the dimensionality of the sensor-level data to this number. We utilized both runs in the MCCA training, by averaging the data matrices $\mathbf{Z}^m$ across the first and second run in calculating the correlation matrix in the MCCA optimization process, as in our previous study (Lankinen et al., 2014). More specifically, the blocks in the correlation matrix $\mathbf{R}$ in MCCA algorithm were

computed as $\mathbf{R}_{ij} = \frac{\overline{\mathbf{X}}_i \overline{\mathbf{X}}_j^T}{N_t - 1}$, where N_t is the number of samples in one trial, and $\overline{\mathbf{X}}_i$, $\overline{\mathbf{X}}_j$ are the average over the subject-wise whitened trials for subject *i* and *j*, ($i \neq j$), respectively.

MCCA was calculated for raw sensor level data, separately for each frequency band studied. We used 10-fold cross-validation for model training and testing. More specifically, the 15-min data were divided to 10 parts, and the model was trained 10 times so that a different non-overlapping segment was used as a test data and the rest as training data. The estimated MCCA coefficients were applied to each test set, and only the concatenated test data were used in further analysis.

For visualization, the weights $\mathbf{W}^m$ $(D \times D)$ were transformed back to the 204 dimensions, $\mathbf{W}'^m$ (204×204), corresponding to the original MEG gradiometer channels. To enable physiological interpretation of the spatial-filter weights, the spatially filtered sensor-level maps need to be further converted to activation patterns (forward models) (Haufe et al. 2014). This procedure refers to finding the activation pattern $\mathbf{A} = \boldsymbol{\Sigma}_z \mathbf{W}'^m \boldsymbol{\Sigma}_y^{-1}$, where $\boldsymbol{\Sigma}_z$ and $\boldsymbol{\Sigma}_y$ are the covariance matrices of the data $\mathbf{Z}^m$ and projections $\mathbf{Y}^m$.

2.5 Correlation analysis

We calculated Pearson's correlation coefficients between the fMRI and MEG signal envelopes at each cortical voxel, separately for each MEG frequency band (see Section 2.4.1). We transformed the cortical fMRI voxel series to the same 'fsaverage' coordinate system as MEG, and picked those voxel time series that corresponded the locations of MEG sources (altogether 5124 locations).

Intrasubject correlation with subject-wise MEG envelopes or fMRI data was computed as a correlation between the time courses between the first and second viewings of the 15-min-long movie at each source or voxel location.

Intersubject correlation was calculated separately for MEG envelopes and fMRI signals, separately for the first and second runs. We first calculated Pearson's correlation coefficient for each subject pair (*i*, *j*) between the 8 subjects (28 combinations). For the second run, one subject had to be excluded from both the MEG and fMRI analyses, resulting in 21 combinations. Next, we applied Fisher's *z*-transformation

$$z_{ij} = \frac{1}{2} ln \frac{(1 + r_{ij})}{(1 - r_{ij})} = \text{atanh}(r_{ij})$$

for each correlation coefficient before computing the mean

$$\bar{z} = \frac{1}{\frac{k^2 - k}{2}} \sum_{i=1}^{k} \sum_{j=2, j>1}^{k} z_{ij}$$

where *k* is the number of subjects. Statistically significant $\bar{z}$-values were transformed back to correlation coefficients by Fisher's inverse *z*-transformation, $r = \tanh(\bar{z})$.

MEG–fMRI correlation was computed between MEG envelopes and fMRI time-courses at corresponding cortical locations, separately for the first and the second run. Before calculating the correlation, the MEG envelope time-courses were convolved with a standard double-gamma hemodynamic response function (*spm_hrf* in SPM8), and fMRI voxel time series were upsampled to 10 Hz to match the sampling rate of the MEG envelopes.

For all the voxel-wise analyses, we used nonparametric circular bootstrapping to find statistically significant correlation coefficients (Chen et al., 2016). To approximate the null distribution, we circularly shifted with random lags the time

series 10 000 times at each voxel and calculated the correlation coefficients for these shifted time series. The *p*-values for the correlation coefficients were estimated from the null distribution. Intrasubject and MEG–fMRI correlation coefficients were tested separately for each subject. For all voxel-wise calculations, the significance threshold was $p < 0.05$, with FDR correction for multiple comparisons.

2.6 Linear modeling between MEG and fMRI

As an alternative approach to assess MEG–fMRI similarities, we first applied spatial-filtering based on MCCA to find consistent MEG time courses across subjects, and then used the envelopes of the resulting MCCA canonical variates as regressors in a general linear model (GLM) to identify similar fMRI time courses.

For each frequency band, we chose the first MCCA canonical variate, corresponding to the strongest intersubject correlation. Next, we averaged these canonical variates across subjects and computed the amplitude envelope (providing information about slow fluctuations of the higher-frequency rhythms) for this averaged time course by Hilbert transform. The resulting signal was further low-pass filtered at 4 Hz, convolved with the canonical hemodynamic response function and resampled to match the sampling rate of fMRI (TR= 2.015).

The GLM analysis was performed using SPM8 package (Wellcome Trust Centre for Neuroimaging; http://www.fil.ion.ucl.ac.u) with the default parameters. Six head-movement signals from the fMRI measurements were included in the design matrix of the GLM-model. The threshold for statistical significance was $p < 0.05$, with FDR-correction.

3 Results

3.1 Intrasubject correlations

Fig. 1 shows the spatial distribution of statistically significant voxel-wise intrasubject correlations between the two runs for one representative subject (subject 6), computed from both the fMRI signals (Fig. 1, top row; for the corresponding results of all subjects, see Supplementary Figure S1) and from MEG signal envelopes divided in 7 frequency bands between 0.03 and 100 Hz (Fig. 1, 7 bottom rows; for the corresponding results of all subjects, see Supplementary Figures S2–S8).

For fMRI, the maximum intrasubject correlation coefficients ranged across subjects from 0.49 to 0.66 (median $r = 0.59$), with the most prominent spatial clusters of high correlation coefficients in occipital areas and smaller clusters in posterior parietal and frontal areas.

MEG intrasubject correlations were also strongest in occipital areas, especially in occipital pole, but they were much weaker (median $r \sim 0.05$–0.14 across frequency bands) and their variation across subjects larger than for fMRI. Generally, the correlation coefficients were lower at higher frequencies, and significant intrasubject correlations were found in most subjects only in bands 1–4 and 4–8 Hz.

3.2 Intersubject correlations

Fig. 2 (top) shows statistically significant average voxel-wise intersubject correlations of fMRI signals between the first runs (see Supplementary Fig. S9 top for the results of the second runs). The highest average intersubject correlation coefficient for fMRI was $r = 0.37$ for the first, and $r = 0.33$ for the second run. The highest

correlation coefficients were found widely in occipital regions, together with weaker correlations in restricted frontal and posterior parietal regions.

Fig. 2 (bottom) shows the statistically significant average intersubject correlations of MEG signal envelopes in each frequency band for the first run (see Supplementary Fig. S9, bottom, for the results for the second run), computed at the same locations in the cortex as for fMRI. The average intersubject correlations were lower for MEG (correlation coefficient $r < 0.05$) than for fMRI signals (correlation coefficient $r \leq 0.37$). In general, the correlation coefficients were smaller the higher the frequency band. The strongest correlations occurred in occipital regions, approximately in the same areas as the strongest correlations in fMRI.

[Figs. 1 and 2 approximately here.]

3.3 MEG–fMRI correlations

Direct voxel-wise MEG–fMRI comparison at the same cortical locations revealed only a few statistically significant correlation coefficients in single subjects for each frequency band, and they were scattered across the cortex. Thus, no reliable correlations were found between fMRI and MEG signal envelopes at the group level.

Supplementary Figure S10 shows an example of actual MEG and fMRI time-courses at voxel where the intersubject correlation for MEG envelopes was the strongest.

3.4 MCCA intersubject correlations

The maximum intersubject correlation between the time series of the first MCCA canonical variates was 0.25 in the < 1-Hz band (for all bands, as well as for

the train and test data results, see Fig. 3). For comparison, the voxel-wise intersubject correlation of MEG envelopes was only 0.03 in the same band (see Fig. 2).

Fig. 4B shows an example of raw source level MEG signals (in arbitrary units) in the 1–4-Hz band at the location of the highest intersubject correlation coefficient (0.005 for raw source level signal, and 0.02 for envelopes (see Fig.2) (Fig. 4A; blue arrow in the left panel). Fig. 4D illustrates the signals in the same band after MCCA application. The figure demonstrates that the signals are more consistent across the subjects and more structured after MCCA application. Fig. 4C shows the activation map of the spatial-filter of the first MCCA canonical variates in 1–4 Hz band. In practice, large values in the activation map indicate brain areas that contribute most to a certain MCCA canonical variate. The activation maps for all the frequency bands are shown in Supplementary Fig. S11.

[Figs. 3 and 4 approximately here.]

3.5 GLM analysis between MEG and fMRI

Finally, the GLM analysis revealed the cortical locations where envelopes of MEG MCCA canonical variates were associated with the fMRI data (Fig. 5). The best fit between the fMRI voxel time series and the MEG-derived regressor occurred in each frequency band (except 13–23 Hz) in occipital regions, excluding the occipital pole. Associations between MEG and fMRI were also found in frontal and temporal regions at frequencies below 8 Hz and at 55–100 Hz.

[Fig. 5 approximately here.]

Fig. 6 (top) shows the spatial distribution of the highest beta-values from the GLM analysis for frequency band 1–4 Hz, demonstrating that the location of the best GLM fit between MEG envelopes and fMRI (in occipital regions except the occipital

pole) differs from the location of the strongest MEG intersubject correlations (in occipital pole; see Fig. 2 bottom) of the same frequency band. Fig. 6 (bottom) shows the fMRI and MEG regressor time courses for the same frequency band at this location.

[Fig. 6 approximately here.]

4 Discussion

We conducted a systematic intra- and intersubject correlation analysis of fMRI and MEG signals collected from participants who were viewing the same 15-min movie altogether 4 times: first 2 times during fMRI scanning and then 2 times during MEG recording. The conventional way of correlating brain signals at each voxel uncovered statistically significant intra- and intersubject correlations between the brain-signal time series when fMRI and MEG data were analyzed separately. However, this voxel-wise correlation approach did not reveal associations between the two imaging methods. Both intra- and intersubject voxel-wise correlation coefficients were considerably lower for MEG than fMRI. However, the intra- and intersubject correlations of the MCCA-derived canonical variates for MEG were much stronger in bands below 8 Hz. Using these variates as regressors to model the fMRI signals revealed also similarities between MEG and fMRI time courses mostly in occipital regions, with smaller clusters in temporal and frontal brain areas.

4.1 Univariate correlations

Both the relatively strong fMRI *intra*subject correlations and the clearly weaker fMRI *inter*subject correlations are in line with previous fMRI studies on movie viewing (Hasson et al., 2004; Golland et al., 2007; Jääskeläinen et al., 2008; Kauppi et

al., 2010; Nummenmaa et al., 2012; Andric et al., 2016). The statistically significant intrasubject and intersubject correlations were found mainly in occipital brain regions. However, the lack of statistically significant correlations in temporal areas can be explained by the absence of any soundtrack in our film. The slightly weaker intersubject correlations during the second than the first viewing can be due to stimulus repetition as has been observed previously (EEG: Dmochowski et al., 2012; fMRI: Lahnakoski et al., 2014), but opposite effect has also been reported (EEG: Chang et al., 2015). It is also noteworthy to remark that the subjects had already seen the movie twice (during fMRI recording) before the first MEG run, which may have further decreased the MEG intersubject correlations. However, given the long time between fMRI and MEG measurements, as well as the very complex nature of the stimulus and the lack of dramatic narrative content, it is unlikely that stimulus repetition effects would have significantly affected the analysis results.

But why were the univariate inter- and intrasubject correlations of MEG signals so modest? Technical reasons include spatial inaccuracies that cannot be avoided in the conversion of the MEG sensor-space signals to MNE source estimates. Moreover, correlations are sensitive to subtle temporal differences in the time courses. The decreasing intra- and intersubject correlation coefficients with increasing frequency in MEG were most likely due to generally smaller signal amplitudes and larger phase differences at higher frequencies. Thus, one likely contributing factor to the weaker intra- and intersubject correlations in MEG than fMRI signals is the more complex nature of the MEG signal that comprises a multitude of different frequencies, each with their own reactivity patters. In addition, because of the high temporal precision of MEG, the brain activity between subjects would need to be very accurately synchronized to yield correlations up to those seen in fMRI, where the brain responses

are temporally smoothed. Furthermore, the frequency contents of MEG brain rhythms likely vary considerably across individuals which further decreases the intersubject correlation values. Of course, alternative MEG processing streams, e.g. a different source estimation technique, could yield higher univariate intra- or intersubject correlation values. However, the minimum-norm estimation is widely used, and it needs minimal prior information of the sources.

4.2 Multivariate modeling

4.2.1 Advantages of MCCA

Our MCCA-based spatial-filtering approach was able to improve the consistency in MEG signals with respect to voxel-wise ISC analysis. A major advantage of the MCCA approach is that it attempts to maximize correlations of sensor-space signals in a data-driven manner, without assumptions about anatomical correspondence. Therefore, differences in head size, orientation, or functional anatomy are not critical. Moreover, MCCA provides a convenient way for sensor-level analysis.

4.2.2 GLM modeling

The envelopes of MEG canonical variates associated with fluctuations in the fMRI voxel time series in the occipital (excluding occipital pole), temporal and frontal brain regions. These regions do not entirely overlap with the areas showing the strongest intersubject correlations in the voxel-wise analysis, especially in MEG where the strongest correlations were found in occipital pole. This finding suggests

that the regions of the most consistent MEG activity might differ from the regions of most correlated fMRI activity across the subjects.

4.3 Neurophysiological differences between MEG and fMRI

Although we found statistically significant intra- and intersubject correlations approximately at the same brain areas separately for fMRI and MEG, only a few scattered voxel-wise MEG–fMRI correlations were found in single subjects. Discrepancies in the locations and temporal dynamics between the MEG and fMRI signals were expected because of the differences in the physiological origins of these signals as well as the inter-regional variation of neurovascular coupling.

Although neural processes with both kinds of temporal dynamics are usually triggered by a single stimulus event, these processes may take place in different cortical locations, which could explain the spatial differences when correlating MEG and fMRI results. Notably, the voxel-wise MEG–fMRI analysis was based strongly on the assumption of anatomical correspondence between the origins of the signals, which leads to weak correlations if the MEG and fMRI signals originate from even slightly different locations. Our analysis is related to functional alignment, used e.g. in Haxby et al. (2011) and Yamada et al. (2015).

Even with accurate spatial alignment, combining the information from MEG and fMRI recordings is not straightforward. MEG signal is rich in information content, with different frequency bands reflecting different brain processes or reacting to different types of stimuli (for a review, see e.g. Hari and Puce, 2017). Single stimuli can elicit in MEG evoked (or event-related) responses in addition to oscillatory activity. In addition, short-lasting activation detected by MEG may go undetected in fMRI (e.g. Furey et al., 2006). Furthermore, the hemodynamic response can vary

between individuals and between brain areas (Handwerker et al., 2004), and thus the canonical HRF used here in fMRI analysis might not be optimal to describe the brain response to a single stimulus.

Previous studies using invasive recordings have demonstrated that the BOLD signal correlates positively with the signal power of high-frequency local field potentials (LFPs) measured from both auditory cortex (Mukamel et al., 2005; Nir et al., 2007) and visual cortex (Privman et al., 2007) during movie viewing. In addition, the signal power of low-frequency LFPs correlated negatively with BOLD signal (Mukamel et al., 2005). These studies have demonstrated that very local electrophysiological activity may couple to hemodynamic activity.

In contrast to our current approach, the relationship between BOLD and MEG/EEG signals has previously been studied in rather well controlled experimental settings, except in resting-state studies in rats and humans (e.g. Bruyns-Haylett et al., 2013; Tewarie et al., 2014). Correlations have been demonstrated between BOLD signals and task-induced changes in the oscillatory power of different frequency bands of the MEG signal, as well as between BOLD responses and MEG evoked responses (for a review, see e.g. Hall et al., 2014). Overall, MEG and fMRI signals display a relatively good spatial agreement in low-level sensory projection areas (e.g. Moradi et al., 2003; Brookes et al., 2005; Nangini et al., 2009; Stevenson et al., 2011) whereas the MEG and fMRI spatial patterns often differ during cognitive tasks (e.g. more than 15 mm in various regions as shown by Liljeström et al., 2009; more than 10 mm outside occipital cortex; Vartiainen et al., 2011). Moreover, the association between BOLD and MEG signals can be region- and frequency-dependent (Kujala et al., 2014) as well as task-related (Furey et al. 2006).

Earlier comparisons between MEG/EEG and fMRI during movie viewing have demonstrated an association between source-level EEG activity (0.5–45 Hz) and BOLD signal with a ~5-s delay that was calculated only in the primary visual cortex (V1) by using a 2-min movie clip presented 25 times (Whittingstall et al., 2010). In a study using of 30-s video clips of Superbowl advertisements as stimuli, the level of intersubject correlation of EEG signals covaried with the amount of BOLD activity in temporal regions, precuneus and medial prefrontal cortex (Dmochowski et al., 2014). Furthermore, 5-min movie clips were used to compare changes of functional connectivity as reflected in MEG and fMRI signals during movie viewing versus resting state (Betti et al., 2013). The current study extends these findings by providing a systematic comparison of unaveraged 15-min MEG and fMRI signals.

4.4 Relationship between brain activity and movie content

Viewing of the same film can be assumed to elicit highly similar sensory and relatively similar cognitive responses across trials and participants, as the events in the film unfold in a similar manner at each viewing. One may thus expect the similarity of the responses be high in the extrinsic and less similar in the intrinsic brain networks (Golland et al., 2007, 2008). Accordingly, in our analysis, the occipital brain regions showing replicable intersubject MEG and fMRI correlations were consistent with the extrinsic brain network reflecting stimulus-driven brain activity. Although we did not study the relationship between the movie content and brain signals, finding—as the first step—consistent features in the complex brain data using MCCA provides a good starting point for further analysis.

5 Conclusions

Our results show that the similarities between MEG and fMRI responses to a continuous naturalistic stimulus cannot be characterized robustly with the commonly used univariate voxel-wise correlation approach, where temporally correlated activations are assumed to occur at the same anatomical locations. However, using a multivariate MCCA-based spatial-filtering approach significantly increased the MEG intersubject correlations. Furthermore, combining the envelopes of the MEG canonical variates with fMRI signals in GLM indicated similarities in time courses in occipital, temporal and frontal brain regions.

6 Acknowledgements

This work has been supported by Finnish Cultural Foundation, Jenny and Antti Wihuri Foundation, Finnish Concordia Fund Grant to KL, Finnish Cultural Foundation Eminentia Grant from Ester and Uuno Kokki Fund to RH, Jane and Aatos Erkko Foundation Grant to MK, and Aalto Starting Grant to PT and YH. We thank Matti Hämäläinen, Emma Suppanen and Anja Thiede for useful suggestions and discussions. We also acknowledge Aalto Science-IT, Aalto Brain Centre (ABC), and Aalto NeuroImaging infrastructure for providing support and facilities for measurements and analysis.

7 References

Andric, M., Goldin-Meadow, S., Small, S.L., Hasson, U., 2016. Repeated movie viewings produce similar local activity patterns but different network configurations. Neuroimage 142, 613–627.

Bartels, A., Zeki, S., 2004a. The chronoarchitecture of the human brain—natural viewing conditions reveal a time-based anatomy of the brain. Neuroimage 22, 419–433.

Bartels, A., Zeki, S., 2004b. Functional brain mapping during free viewing of natural scenes. Hum. Brain Mapp. 21, 75–85.

Betti, V., Della Penna, S., de Pasquale, F., Mantini, D., Marzetti, L., Romani, G.L., Corbetta, M., 2013. Natural scenes viewing alters the dynamics of functional connectivity in the human brain. Neuron 79, 782–797.

Bridwell, D.A., Roth, C., Gupta, C.N., Calhoun, V.D., 2015. Cortical response similarities predict which audiovisual clips individuals viewed, but are unrelated to clip preference. PloS One 10(6), e0128833.

Brookes, M.J., Gibson, A.M., Hall, S.D., Furlong, P.L., Barnes, G.R., Hillebrand, A., Singh, K.D., Holliday, I.E., Francis, S.T., Morris, P. G., 2005. GLM-beamformer method demonstrates stationary field, alpha ERD and gamma ERS co-localisation with fMRI BOLD response in visual cortex. Neuroimage 26, 302–308.

Bruyns-Haylett, M., Harris, S., Boorman, L., Zheng, Y., Berwick, J., Jones, M., 2013. The resting-state neurovascular coupling relationship: rapid changes in spontaneous neural activity in the somatosensory cortex are associated with haemodynamic fluctuations that resemble stimulus-evoked haemodynamics. Eur. J. Neurosci. 38,2902–2916.

Chang, W.T., Jääskeläinen, I.P., Belliveau, J.W., Huang, S., Hung, A.Y., Rossi, S., Ahveninen, J., 2015. Combined MEG and EEG show reliable patterns of electromagnetic brain activity during natural viewing. Neuroimage 114, 49–56.

Chen, G., Shin, Y.W., Taylor, P.A., Glen, D.R., Reynolds, R.C., Israel, R.B., Cox, R.W., 2016. Untangling the relatedness among correlations, part I: Nonparametric approaches to inter-subject correlation analysis at the group level. Neuroimage 142, 248–259.

Cohen, S.S., Parra, L.C., 2016. Memorable audiovisual narratives synchronize sensory and supramodal neural responses. eNeuro 3, 1–11.

Correa, N.M., Adali, T., Li, Y.O., Calhoun, V.D., 2010. Canonical correlation analysis for data fusion and group inferences. IEEE Signal Process. Mag. 27 (4), 39–50.

Dale, A.M., Fischl, B., Sereno, M.I., 1999. Cortical surface-based analysis. I. Segmentation and surface reconstruction. Neuroimage 9, 179–194.

Dmochowski, J.P., Sajda, P., Dias, J., Parra, L.C., 2012. Correlated components of ongoing EEG point to emotionally laden attention-a possible marker of engagement? Front. Hum. Neurosci. 6, 112.

Dmochowski, J.P., Bezdek, M.A., Abelson, B.P., Johnson, J.S., Schumacher, E.H., Parra, L.C., 2014. Audience preferences are predicted by temporal reliability of neural processing. Nature Communic., 5.

Dähne, S., Bießmann, F., Samek, W., Haufe, S., Goltz, D., Gundlach, C., Villringer, A., Fazli, S., Müller, K.R., 2015. Multivariate machine learning methods for fusing multimodal functional neuroimaging data. Proc. IEEE 103, 1507–1530.

Fischl, B., Sereno, M., Dale, A., 1999a. Cortical surface-based analysis ii: inflation, flattening, and a surface-based coordinate system. Neuroimage 9, 195–207.

Fischl, B., Sereno, M.I., Tootell, R.B., Dale, A.M., 1999b. High-resolution intersubject averaging and a coordinate system for the cortical surface. Hum. Brain Mapp. 8, 272–284.

Furey, M.L., Tanskanen, T., Beauchamp, M.S., Avikainen, S., Uutela, K., Hari, R., Haxby, J.V., 2006. Dissociation of face selective cortical responses by attention. Proc. Natl. Acad. Sci. U.S.A. 103, 1065–1070.

Golland, Y., Bentin, S., Gelbard, H., Benjamini, Y., Heller, R., Nir, Y., Hasson, U., Malach, R., 2007. Extrinsic and intrinsic systems in the posterior cortex of the human brain revealed during natural sensory stimulation. Cereb. Cortex 17, 766–777.

Golland, Y., Golland, P., Bentin, S., Malach, R., 2008. Data-driven clustering reveals a fundamental subdivision of the human cortex into two global systems. Neuropsychologia 46, 540–553.

Gramfort, A., Luessi, M., Larson, E., Engemann, D. A., Strohmeier, D., Brodbeck, C., Parkkonen, L., Hämäläinen, M.S., 2014. MNE software for processing MEG and EEG data. Neuroimage 86, 446–460.

Hall, E.L., Robson, S.E., Morris, P.G., Brookes, M.J., 2014. The relationship between MEG and fMRI. Neuroimage 102, 80–91.

Handwerker, D.A., Ollinger, J.M., D'Esposito, M., 2004. Variation of BOLD hemodynamic responses across subjects and brain regions and their effects on statistical analyses. Neuroimage 21, 1639–1651.

Hari, R., 2007. How to image the human brain. In M. Klockars, & M. Peltomaa (Eds.), Acta Gyllenbergiana VII: Music Meets Medicine (pp. 49–61). Helsinki: The Signe and Ane Gyllenberg Foundation.

Hari, R., Kujala, M.V., 2009. Brain basis of human social interaction: from concepts to brain imaging. Physiological reviews 89, 453–479.

Hari, R., Parkkonen, L., 2015. The brain timewise: how timing shapes and supports brain function. Phil. Trans. R. Soc. Lond. B Biol. Sci. 370, 20140170.

Hari, R., Puce, A., 2017. MEG-EEG Primer. Oxford University Press.

Hasson, U., Nir, Y., Levy, I., Fuhrmann, G., Malach, R., 2004. Intersubject synchronization of cortical activity during natural viewing. Science 303, 1634–1640.

Hasson, U., Yang, E., Vallines, I., Heeger, D.J., Rubin, N., 2008. A hierarchy of temporal receptive windows in human cortex. J. Neurosci. 28, 2539–50.

Hasson, U., Malach, R., Heeger, D.J., 2010. Reliability of cortical activity during natural stimulation. Trends Cogn. Sci. 14, 40–48.

Haufe, S., Meinecke, F., Görgen K., Dähne, S., Haynes, J.D., Blankertz, B., Bießmann F., 2014. On the interpretation of weight vectors of linear models in multivariate neuroimaging. Neuroimage 87: 96–110.

Haxby, J.V., Guntupalli, J.S., Connolly, A.C., Halchenko, Y.O., Conroy, B.R., Gobbini, M.I., Ramadge, P.J., 2011. A common, high-dimensional model of the representational space in human ventral temporal cortex. Neuron 72:404–416.

Hämäläinen, M.S., Ilmoniemi, R.J., 1994. Interpreting magnetic fields of the brain: minimum norm estimates. Med. Biol. Eng. Comput. 32, 35–42.

Jääskeläinen, I.P., Koskentalo, K., Balk, M.H., Autti, T., Kauramäki, J., Pomren, C., Sams, M., 2008. Inter-subject synchronization of prefrontal cortex hemodynamic activity during natural viewing. Open Neuroimaging J. 2, 14–19.

Kauppi, J.-P., Jääskeläinen, I.P., Sams, M., Tohka, J., 2010. Inter-subject correlation of brain hemodynamic responses during watching a movie: localization in space and frequency. Front. Neuroinform. 4 (5).

Kauppi, J.P., Pajula, J., Niemi, J., Hari, R., Tohka, J., 2017. Functional brain segmentation using inter-subject correlation in fMRI. Hum. Brain Mapp. 385, 2643–2665.

Kauttonen, J., Hlushchuk, Y., Tikka, P., 2015. Optimizing methods for linking cinematic features to fMRI data. Neuroimage 110, 136–148.

Kettenring, J.R., 1971. Canonical analysis of several sets of variables. Biometrika 58, 433–451.

Ki, X.J.J., Kelly, S.P., Parra, L.C., 2016. Attention Strongly Modulates Reliability of Neural Responses to Naturalistic Narrative Stimuli J. Neurosci. 36, 3092–3101.

Kujala, J., Sudre, G., Vartiainen, J., Liljeström, M., Mitchell, T., Salmelin, R., 2014. Multivariate analysis of correlation between electrophysiological and hemodynamic responses during cognitive processing. Neuroimage 92, 207–216.

Lahnakoski, J.M., Salmi, J., Jääskeläinen, I.P., Lampinen, J., Glerean, E., Tikka, P., Sams, M., 2012. Stimulus-related independent component and voxel-wise analysis of human brain activity during free viewing of a feature film. PLoS ONE 7, e35215.

Lahnakoski, J.M., Glerean, E., Jääskeläinen, I.P., Hyönä, J., Hari, R., Sams, M., Nummenmaa, L., 2014. Synchronous brain activity across individuals underlies shared psychological perspectives. Neuroimage 100, 316–324.

Lankinen, K., Saari, J., Hari, R., Koskinen, M., 2014. Intersubject consistency of cortical MEG signals during movie viewing. Neuroimage 92, 217–224.

Lankinen, K., Smeds, E., Tikka, P., Pihko, E., Hari, R., Koskinen, M., 2016. Haptic contents of a movie dynamically engage the spectator’s sensorimotor cortex. Hum. Brain Mapp. 37, 4061–4068.

Li, Y.O., Adali, T., Wang, W., Calhoun, V.D., 2009. Joint blind source separation by multi-set canonical correlation analysis. IEEE Trans. Signal Process. 57, 3918–3929.

Logothetis, N.K., Pauls, J., Augath, M., Trinath, T., Oeltermann, A., 2001. Neurophysiological investigation of the basis of the fMRI signal. Nature 412, 150–7.

Moradi, F., Liu, L.C., Cheng, K., Waggoner, R.A., Tanaka, K., Ioannides, A.A., 2003. Consistent and precise localization of brain activity in human primary visual cortex by MEG and fMRI. Neuroimage 18, 595–609.

Mukamel, R., Gelbard, H., Arieli, A., Hasson, U., Fried, I., Malach, R., 2005. Coupling between neuronal firing, field potentials, and FMRI in human auditory cortex. Science 309, 951–954.

Nangini, C., Hlushchuk, Y., Hari, R., 2009.Predicting stimulus-rate sensitivity of human somatosensory fMRI signals by MEG. Hum. Brain Mapp. 30, 1824–1832.

Nir, Y., Fisch, L., Mukamel, R., Gelbard-Sagiv, H., Arieli, A., Fried, I., Malach, R., 2007. Coupling between neuronal firing rate, gamma LFP, and BOLD fMRI is related to interneuronal correlations. Curr. Biol. 17, 1275–1285.

Nummenmaa, L., Glerean, E., Viinikainen, M., Jääskeläinen, I.P., Hari, R., Sams, M., 2012. Emotions promote social interaction by synchronizing brain activity across individuals. Proc. Natl. Acad. Sci. U.S.A. 109, 9599–9604.

Pamilo, S.,Malinen, S., Hlushchuk, Y., Seppä, M., Tikka, P., Hari, R., 2012. Functional subdivision of group-ICA results of fMRI data collected during cinema viewing. PLoS ONE 7, e42000.

Privman, E., Nir, Y., Kramer, U., Kipervasser, S., Andelman, F., Neufeld, M. Y., Mukamel, R., Yeshurun, Y., Fried, I., Malach, R., 2007. Enhanced category tuning revealed by intracranial electroencephalograms in high-order human visual areas. The

J. Neurosci. 27, 6234–6242. Segonne, F., Dale, A.M., Busa, E., Glessner, M., Salat, D., Hahn, H.K., Fischl, B., 2004. A hybrid approach to the skull stripping problem in MRI. Neuroimage 22, 1060–1075.

Stevenson, C.M., Brookes, M.J., Morris, P.G., 2011. ß-Band correlates of the fMRI BOLD response. Hum. Brain Mapp. 32, 182–197.

Suppanen, E., 2014. Inter-subject correlation of MEG data during movie viewing. Master's thesis, Aalto University.

Taulu, S., Kajola, M., 2005. Presentation of electromagnetic multichannel data: the signal space separation method. J. Appl. Phys. 97 (124905), 1–10.

Tewarie, P., Hillebrand, A., van Dellen, E., Schoonheim, M.M., Barkhof, F., Polman, C.H., Beaulieu, C., Gong, G., van Dijk, B.W., Stam, C.J., 2014. Structural degree predicts functional network connectivity: A multimodal resting-state fMRI and MEG study. NeuroImage 97, 296–307.

Vartiainen, J., Liljeström, M., Koskinen, M., Renvall, H., Salmelin, R., 2011. Functional magnetic resonance imaging blood oxygenation level-dependent signal and magnetoencephalography evoked responses yield different neural functionality in reading. J. Neurosci. 31, 1048–1058.

Whittingstall, K., Bartels, A., Singh, V., Kwon, S., Logothetis, N.K., 2010. Integration of EEG source imaging and fMRI during continuous viewing of natural movies. Magn. Reson. Imaging 28, 1135–1142.

Yamada, K., Miyawaki, Y., Kamitani, Y., 2015. Inter-subject neural code converter for visual image representation. Neuroimage 113:289–297.

8 Figure legends

Figure 1. Intrasubject correlations between two runs. Top: fMRI results for one representative subject. Bottom: Intrasubject correlations of MEG envelopes for the same subject in all frequency bands. Only statistically significant correlation coefficients are shown. The maximum values of correlation coefficients for each frequency band are shown on the right side of the figure.

Figure 2. Intersubject correlations for fMRI and MEG for the first run. Top: fMRI intersubject correlations. Bottom: Intersubject correlations of MEG envelopes for all frequency bands. Only statistically significant correlation coefficients are shown. The maximum values of correlation coefficients for each frequency band are shown on the right side of the figure.

Figure 3. MCCA train and test data. Pair-wise calculated intersubject correlations of MCCA canonical variates in frequency bands tested. Distributions of correlation coefficients are layed over a box covering 1 SD, and white stripes shows the mean of the data. Gray boxes show train data, and black boxed test data.

Figure 4. Comparison of MEG voxel-wise time series and MCCA canonical variates. (A) Location of highest intersubject correlation coefficient in the band 1–4 Hz (blue arrow). (B) Example of MEG signals (black, mean with red, arbitrary units) from all 8 subjects in the same band (first run) before MCCA at the location of highest intersubject correlation coefficient. (C) Activation map (arbitrary units) from spatial filtering with MCCA in the band 1–4 Hz. (D) Signals from all the subjects after applying MCCA (black, mean with magenta, arbitrary units) in the same band.

Figure 5. GLM fit between MEG and fMRI. Results from GLM fit between the envelopes of MEG MCCA canonical variates and fMRI data in different frequency bands (beta values, arbitrary units).

Figure 6. Time courses of the most similar MEG and fMRI signals. Top: Location of largest beta-value from SPM GLM analysis (blue arrow). Bottom: MEG regressor in the band 1–4 Hz (envelopes of first MCCA canonical variate, red, arbitrary units) and fMRI signal (black, arbitrary units) time courses at the same location.

Supplementary Figure S1. fMRI intrasubject correlations. Intrasubject correlation for fMRI between the first and the second run for all the subjects. Only statistically significant correlation coefficients are shown.

Supplementary Figure S2. MEG intrasubject correlations in band 0.03–1 Hz. Intrasubject correlations for MEG envelopes between the first and the second run for all the subjects in frequency band 0.03–1 Hz. Only statistically significant correlation coefficients are shown.

Supplementary Figure S3. MEG intrasubject correlations in band 1–4 Hz. Intrasubject correlations for MEG envelopes between the first and the second run for all the subjects in frequency band 1–4 Hz. Only statistically significant correlation coefficients are shown.

Supplementary Figure S4. MEG intrasubject correlations in band 4–8 Hz. Intrasubject correlations for MEG envelopes between the first and the second run for all the subjects in frequency band 4–8 Hz. Only statistically significant correlation coefficients are shown.

Supplementary Figure S5. MEG intrasubject correlations in band 8–11 Hz. Intrasubject correlations for MEG envelopes between the first and the second run for all the subjects in frequency band 8–11 Hz. Only statistically significant correlation coefficients are shown.

Supplementary Figure S6. MEG intrasubject correlations in band 13–23 Hz. Intrasubject correlations for MEG envelopes between the first and the second run for all the subjects in frequency band 13–23 Hz. Only statistically significant correlation coefficients are shown.

Supplementary Figure S7. MEG intrasubject correlations in band 25–45 Hz. Intrasubject correlations for MEG envelopes between the first and the second run for all the subjects in frequency band 25–45 Hz. Only statistically significant correlation coefficients are shown.

Supplementary Figure S8. MEG intrasubject correlations in band 55–100 Hz. Intrasubject correlations for MEG envelopes between the first and the second run for all the subjects in frequency band 55–100 Hz. Only statistically significant correlation coefficients are shown.

Supplementary Figure S9. Intersubject correlations for fMRI and MEG for the second run. Top: fMRI intersubject correlations. Bottom: MEG intersubject correlations for all frequency bands. Only statistically significant correlation coefficients are shown. The maximum values of correlation coefficients for each frequency band are shown on the right side of the figure.

Supplementary Figure S10. Comparison of MEG and fMRI voxel-wise time series. Top: MEG signal envelopes convolved with HRF (black, mean with red, arbitrary units) from all 8 subjects in the band 1–4 Hz (first run) in the voxel (right) that showed the highest MEG intersubject correlation coefficient (0.02). Middle: fMRI signal (black, mean with red, arbitrary units) from all 8 subjects (first run) at the same location. Intersubject correlation of the signals is 0.14. Bottom: Averages of the MEG (black) and fMRI (red) signals in top and middle plots at the same locations. Correlation between the signals is 0.11. The signals are scaled to the same units (zero mean, variance 1).

Supplementary Figure S11. Activation maps from spatial filtering. The activation maps from the MCCA spatial filters for each frequency band (arbitrary units and signs).